Available online at www.sciencedirect.com
ScienceDirect
Journal of Nuclear Materials 359 (2006) 102–113
journal of nuclear materials
www.elsevier.com/locate/jnucmat

Electrochemical reduction of (U–40Pu–5Np)O_2 in molten LiCl electrolyte

Masatoshi Iizuka *, Yoshiharu Sakamura, Tadashi Inoue

Central Research Institute of Electric Power Industry, Nuclear Technology Research Laboratory, Iwato-kita 2-11-1, Komae, Tokyo 201-8511, Japan

Received 5 April 2006; accepted 11 August 2006

Abstract

The electrochemical reduction of neptunium-containing MOX ((U–40Pu–5Np)O_2) was performed in molten lithium chloride melt at 923 K to investigate fundamental behavior of the transuranium elements and applicability of the method to reduction process for these materials. The Np-MOX was electrochemically reduced at the potential lower than −0.6 V vs. Bi–35 mol% Li reference electrode. The reduced metal grains in the surface region of the sample cohered with each other and made the layer of relatively high density, although it did not prevent the reduction of the sample toward the center. Complete reduction of the Np-MOX was shown by the weight change measurement through the electrochemical reduction and also by SEM–EDX observation. The chemical composition of the reduction products was homogeneous and agreed to that of the initial Np-MOX, which indicates that the reduction was completed and not selective among the actinides. The concentrations of the actinide elements, especially plutonium and americium in the electrolyte, increased with the progress of the tests, although their absolute values were very small. It is quite likely that plutonium and americium dissolve into the melt in the same manner as the lanthanide elements in the lithium reduction process.

PACS: 28.41.Bm; 82.45.Hk; 82.80.Fk

1. Introduction

Development of innovative nuclear fuel cycle technology is strongly expected to secure an effectual measure for improvement in the environmental sustainability and answer to the increasing energy demand. Central Research Institute of Electric Power Industry proposes the metallic fuel cycle as one of the most promising options in the next generation nuclear fuel cycle technologies. The metallic fuel cycle, a combination of the metal fuel fast reactor and the pyrometallurgical reprocessing, has excellent advantages in economic, safety and proliferation resistance aspects [1].

Since the oxide fuel is used in the current light water reactors, it is needed to reduce the oxide in order to obtain the material for the introduction of the metal fuel fast reactors. The reduction method can be applied either to the uranium–plutonium mixed oxide product from LWR fuel

* Corresponding author. Tel.: +81 3 3480 2111; fax: +81 3 3480 7956.
E-mail address: iizuka@criepi.denken.or.jp (M. Iizuka).

0022-3115/$ - see front matter © 2006 Elsevier B.V. All rights reserved.
doi:10.1016/j.jnucmat.2006.08.003

reprocessing, or to the LWR spent fuels. In the latter case, pyrometallurgical processes, such as the molten salt electrorefining process [2] should follow the reduction step for removal of the fission product elements.

The lithium reduction process using lithium metal reductant in molten lithium chloride bath has been developed for that purpose. Reduction of UO_2 [3] and simulated spent LWR fuel [4] was demonstrated. The thermodynamic conditions for reduction of transuranium elements [5] and the behavior of major fission product elements [6] were also studied. The co-produced Li_2O should be removed from the molten salt bath to prevent the re-oxidation of the reduction product. The lithium reductant was successfully recovered by electrochemical decomposition of the co-produced Li_2O in the bath [7]. Although the lithium reduction process is thus already experimentally proven technique, there are still some technical problems to be solved such as the handling of highly reactive and sticky lithium metal and the difficulties in design of the lithium recovery equipment.

Recently, the electrochemical reduction method has been studied for reduction of oxide nuclear fuels. Fig. 1 shows diagram of the electrochemical reduction process for spent oxide fuels. The cathode and anode reactions are as follows:

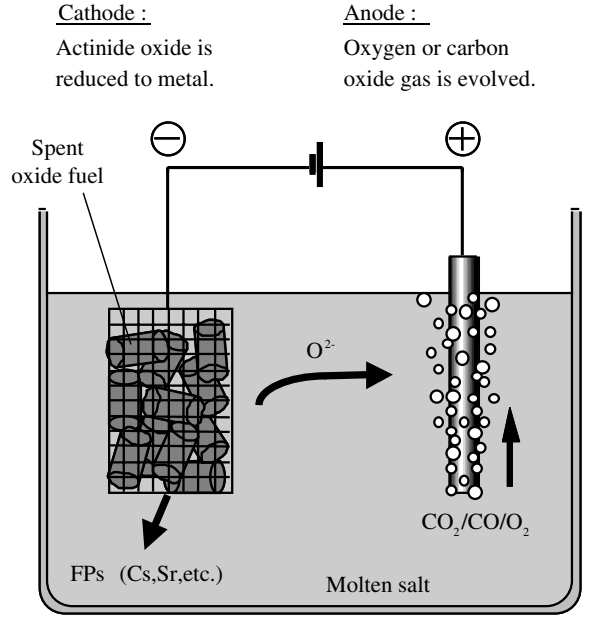

Fig. 1. Schematic diagram of the electrochemical reduction process.

$$\text{Cathode:}\quad MO_2 + 4e^- \rightarrow M + 2O^{2-} \tag{1}$$

$$\text{Anode:}\quad 2O^{2-} \rightarrow O_2 + 4e^- \tag{2}$$

When a carbon anode is used, CO or CO_2 is evolved in place of O_2.

$$\text{Anode:}\quad 2O^{2-} + C \rightarrow CO_2 + 4e^- \tag{3}$$

$$O^{2-} + C \rightarrow CO + 2e^- \tag{4}$$

One of the advantages of the electrochemical reduction process is that there is no troublesome handling of lithium metal. Another advantage is that the oxide ion produced at the cathode is simultaneously consumed at the anode. It means that the concentration of oxide ion in the bath can be maintained at desired low level. This nature of the process is very favorable because low oxide ion concentration thermodynamically pushes the reaction towards complete reduction of the actinide elements. No accumulation of oxide ion in the bath also indicates that there is theoretically no restriction on the amount of the electrolyte contributing to reduction of required volume of the equipment.

Until now, the electrochemical reduction of UO_2 and UO_2–PuO_2 in molten LiCl or $CaCl_2$ bath has been studied [8–10]. In $CaCl_2$ bath at 1123 K, a thin but dense layer formed in the surface region of the oxide materials in the cathode due to cohesion among the reduced uranium metal particles. Since this layer hampered the outward diffusion of oxygen ion evolved by the reaction (1), subsequent reduction was disturbed and the center region of the cathode material remained as the original oxide. In LiCl bath at 923 K, on the other hand, the reduction product did not cohere so much to form a dense layer probably because of lower temperature. Consequently, there was no such a strong barrier for diffusion of oxygen ion as seen in $CaCl_2$, and both UO_2 and UO_2–PuO_2 samples were successfully reduced toward the center.

Thus, the feasibility and desirable conditions for the electrochemical reduction of uranium and plutonium oxides have been experimentally well clarified. In order to evaluate the material balance and establish the process flow sheet, it is necessary to understand the behavior of minor actinide and major fission product elements in the electrochemical reduction process.

In the present study, the electrochemical reduction of $(U–40Pu–5Np)O_2$ was performed in molten lithium chloride melt at 923 K to investigate

fundamental behavior of the transuranium elements (neptunium and americium yielded by β^- decay from Pu^{241}) and applicability of the method to reduction process for these materials.

2. Experimental

2.1. Apparatus

All the electrochemical reduction experiments were carried out in an argon atmosphere glove box, because lithium chloride is highly hygroscopic and the reduction products might be easily re-oxidized even by low concentration of oxygen. The concentration of water in the argon atmosphere was kept lower than 1.0 ppm during the tests by using the purification system. But the oxygen level was much higher (30–60 ppm) during this period due to the deterioration of the copper catalyst. The effect of this level of oxygen was, however, not significant because the reduced cathodes were quickly cooled after completion of the test and stored in the sealed containers until just before analyses.

Fig. 2 shows a schematic view of the experimental apparatus. A MgO crucible (40 mm in inner diameter, 75 mm depth and 5 mm thickness) containing lithium chloride was placed in the stainless steel vessel and heated to 923 K. The temperature was kept ±2 K by a PID controller and occasionally checked with type-K thermocouple covered with MgO tube.

For the basic electrochemical measurement, a tantalum wire working electrode (1 mm diameter and about 20 mm in immersed depth) was used. In the electrochemical reduction experiments, baskets of approximately 10 mm diameter made from Ta mesh and Ta wire were used to hold the small MOX pieces.

As a counter electrode for the electrochemical measurement or an anode for the electrochemical reduction experiments, a platinum wire electrode

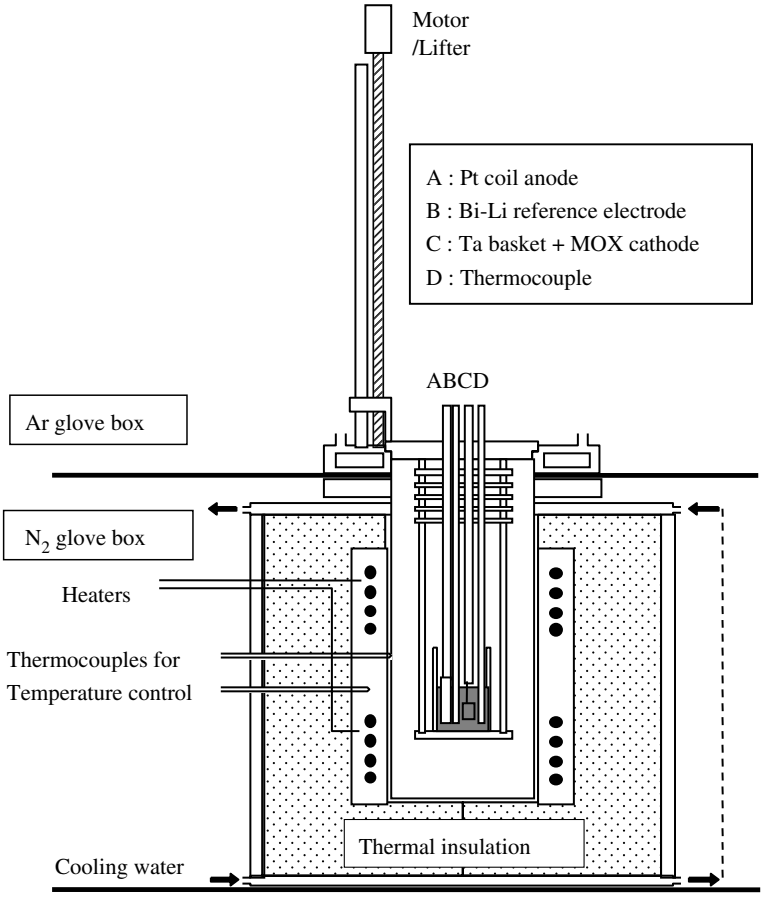

Fig. 2. Schematic view of the experimental apparatus.

was used. The platinum wire of 1 mm diameter was coiled in the shape of 4 mm in diameter and 20 mm in length, and the upper end of the wire was connected to the tantalum wire to make the electric lead. The effective length and the surface area of the platinum wire about 200 mm and 6.3 cm^2, respectively. This platinum anode was then covered with a MgO shroud (6/10 mm in inner/outer diameters) which avoids the decrease of the current efficiency by minimizing the migration of evolving oxygen gas to the cathode.

Bi–Li alloy was used as a reference electrode. About 0.5 g of 35 mol% Li–Bi alloy was put in a MgO tube (4/6 mm in inner/outer diameters) with one end closed. According to the Bi–Li binary phase diagram, this alloy exists as a homogeneous liquid at temperature higher than about 673 K. A tantalum wire of 1 mm in diameter was inserted in the tube as an electric lead. A small hole (0.7 mm in diameter) was made on the wall of the tube at the position between surface levels of the molten lithium chloride and Bi–Li alloy. This hole acts as a very small channel between inside and outside of the MgO tube so that this electrode shows the potential of Li^+/Li redox equilibrium. Theoretically this potential is affected by the change of Li activity in the alloy due to the dissolution into lithium chloride, migration of Li metal produced at the cathode, and so on. In practical, however, this electrode showed stable potential during about one week of the experimental period because of the very small channel.

EG&G Princeton Applied Research Model 263 A with software version 4.0 was used for basic electrochemical measurement such as cyclic voltammetry. For the polarization curve measurement and the electrochemical reduction experiments, a constant electric current was applied with a DC voltage/current generator (ADVANTEST TR6143) and the electrode potentials were measured with digital multimeters (ADVANTEST R8240 and Schlumberger SI7063).

2.2. Chemicals

Lithium chloride of 99.9% purity was purchased from Applied Physical Laboratory, US. It was used without any additional treatment before use since the amount of O_2 and H_2O impurities were extremely low. The concentration of oxide ion O^{2-} in the molten lithium chloride electrolyte is one of the most important parameter affecting the performance of the electrochemical reduction step. The higher O^{2-} concentration gives more abundant supply to the anode and makes it easier to avoid the generation of corrosive Cl_2 gas. At the same time, however, the electrochemical reduction of MOX becomes thermodynamically more difficult at higher O^{2-} concentration. The concentration of O^{2-} in the molten salt electrolyte was adjusted by adding Li_2O of 99.9% purity purchased from Johnson Matthey Co. MgO used as the crucible and the electrode material was 99.9% in purity. All the metals used as the electrode materials were higher than 99.9% in purity.

The nominal composition of the neptunium-containing mixed oxide (called 'Np-MOX' hereafter) pellets used in this study is (U–40Pu–5Np)O_2. They have a hollow shape with central hole of 2.32 mm inner diameter. Other dimensions of the pellets are shown in Table 1. Since these pellets were fabricated by the sol–gel method, they have excellent homogeneity and high density. The ceramographic observation showed that the average grain size of the bulk pellet was around 10 μm. The actual composition analytically determined just after the fabrication is shown in Table 2. Due to the decay, the plutonium and americium contents in this material when it was used in the electrochemical reduction tests are estimated about 2.0% smaller and higher, respectively. One of these pellets was broken into small pieces of 1–3 mm and put in the tantalum basket as described above.

Table 1
Dimension and weight of the (U–40Pu–5Np)O_2 pellet

Pellet no.	Mass (g)	Height (mm)	Diameter (mm)	Density (g/cm^3)	%TD
1	1.4504	7.16	5.43	10.70	95.9
2	1.4525	7.17	5.43	10.70	95.9
3	1.4418	7.09	5.43	10.74	96.2

Table 2
Chemical composition of the (U–40Pu–5Np)O_2 pellet

Element	wt%	mol%
Pu	35.52	40.44
U	47.4	53.96
Np	4.45	5.07
Am	0.461	0.524
Sum of metals	87.831	100
O/M		1.993

2.3. Analytical methods

The molten lithium chloride samples were taken by putting an alumina tube at room temperature quickly into the crucible and by quenching a small amount of the salt on the surface of the tube. The salt samples were analyzed by ICP-MS for their composition. The cathode samples were divided into two portions after washing with methanol to remove the adhering lithium chloride. One was submitted to ICP-MS for chemical composition of the samples. Another portion was polished and analyzed by SEM/EDX for the microstructure and distribution of each actinide in the reduced material.

3. Results and discussion

3.1. Conditions for electrochemical reduction of Np-MOX

Fig. 3 shows the cyclic voltammogram measured in the blank lithium chloride melt with the tantalum wire electrode. There was almost no reduction current between +1.0 V and −0.60 V, indicating the negligible amount of impurities in the salt. The small reduction current at −0.60 V is often observed with tantalum electrode. It is considered to be due to the deoxidization of tantalum, although its effect on the CV is almost negligible. The reduction current increases at potential lower than −0.70 V and showed especially rapid rise near −0.75 V. This current corresponds to the reduction of lithium ($Li^+ + e^- = Li$). After deposition of lithium metal on the surface of the tantalum electrode by imposing a constant reduction current, this electrode also showed a stable potential at $-0.75 \sim -0.76$ V which comes from the Li^+/Li redox pair. Excess amount of lithium metal deposition on the cathode is considered to hamper the diffusion of oxygen ion from the cathode and disturb the progress of the reduction. In the following electrochemical reduction tests, therefore, the cathode potential was kept higher than −0.75 V by adjusting the reduction current.

Fig. 4 shows the cyclic voltammograms measured in lithium chloride melts with the platinum coil electrode. Before addition of Li_2O (curve (a) in Fig. 4), very rapid single increase of the oxidation current is found at potential higher than +2.2 V corresponding to dissolution of platinum: $Pt = Pt^{2+} + 2e^-$. After the addition of Li_2O (curve (b) in Fig. 4), another anodic current peak appeared at +1.9 V. This anodic current is attributed to oxidation of O^{2-} evolving O_2 in the reaction (2). Although it is reported that formation of Li_2PtO_3 occurs at a little lower potential, this reaction was not much remarkable in this voltammogram. From those results, attention was paid to keep the anode potential lower than +2.0 V in order to avoid the loss of platinum by anodic dissolution as much as possible.

In order to determine the appropriate reduction current, current–potentials curves were investigated for the tantalum basket cathode with/without Np-MOX inside it. In the measurement, constant current was added between the cathode and the anode. The potentials were recorded until they showed stable values. In some cases where it took too long time to reach stable potential, however, the measurement was terminated in 4–6 min to avoid large change of the surface conditions of the electrodes. The current was increased stepwise until either of the electrodes reached the limitations determined as shown above, i.e. −0.75 V for the cathode and +2.0 V for the anode.

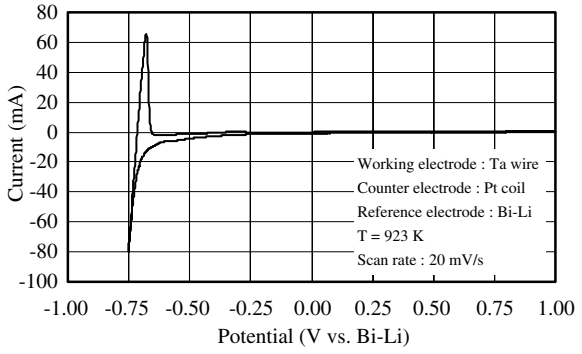

Fig. 3. Cyclic voltammogram measured in the blank lithium chloride melt with the tantalum wire electrode.

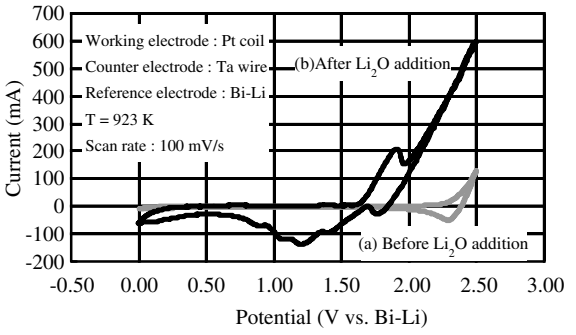

Fig. 4. Cyclic voltammograms measured in lithium chloride melts with the platinum coil electrode.

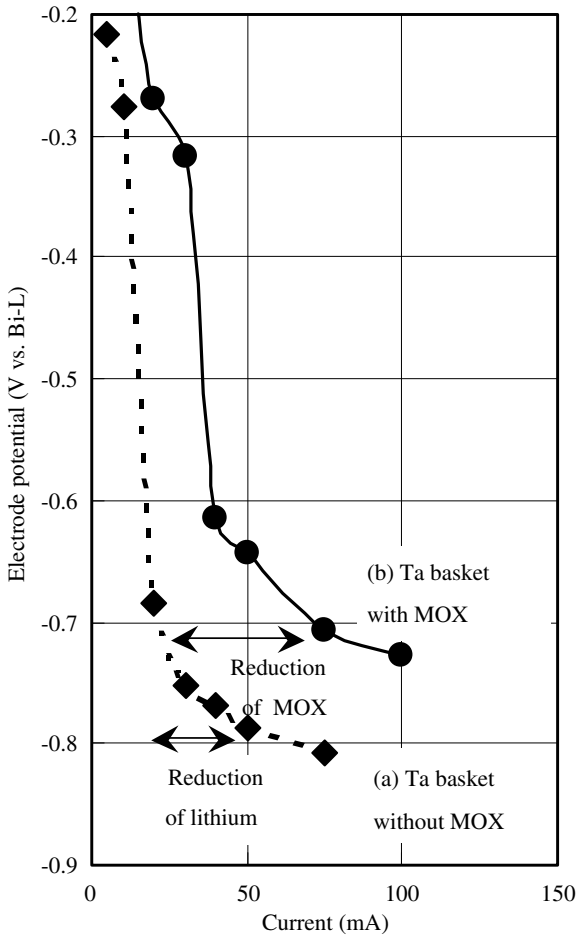

Fig. 5. Current–potentials curves with the Ta basket cathode with/without the MOX.

Fig. 5 shows the measured current–potential curves. Without the MOX in the cathode basket (curve (a)), the reduction current is very small at potential higher than −0.75 V and it rapidly increases with decreasing the potential from around −0.75 V due to the reduction of lithium. This behavior well agrees with the cyclic voltammogram shown in Fig. 3. When some pieces of the Np-MOX (0.891 g in total) are loaded in the basket (curve (b)), the reduction current clearly increases from around −0.6 V, which is much higher potential than that in the case without MOX. This difference is properly due to the electrochemical reduction of the MOX. From these curves, it was also expected that reduction current of around 75 mA would be attainable at least in the early part of the electrochemical reduction under these conditions.

3.2. Change of anode/cathode potentials during electrochemical reduction

Two series of electrochemical reduction tests were carried out to investigate the behavior and the attainable reduced ratio of the transuranium elements. The major parameters of these tests are shown in Table 3. The initial applied current and the limiting anode/cathode potentials are determined from the results of the above current–potential curves measurement and cyclic voltammetry, respectively.

According to the progress of electrochemical reduction, the cathode potential gradually declines. When it reached around −0.75 V, where lithium in the electrolyte is reduced to its metal, the electrolytic current was lowered in stepwise manner to wholly reduce the Np-MOX while avoiding deposition of significant amount of lithium.

Fig. 6 shows the change of the cathode potential during the second electrochemical reduction test. The electric charge passed between the electrodes is taken as the horizontal axis in order to indicate the progress of the reduction process more quantitatively. After the first step at 75 mA, where about the same amount of electric charge as that theoretically required for complete reduction of the loaded MOX was passed, the cathode potential quickly went down in most of the subsequent steps even at smaller reduction current. This result suggests that the electrochemical reduction of the MOX was almost

Table 3
Major parameters in the electrochemical reduction tests

Run no.	Amount of MOX loaded in cathode (g)	Li_2O concentration (wt%)	Current (mA)[a]	Total electric charge (coulomb)	Total electric charge/loaded amount of MOX (%)[b]
1	0.3270	0.51	50–10	1201	257
2	0.8906	0.51	75–5	1725	134

[a] The current was gradually lowered to avoid the reduction of lithium.
[b] The ratio between the total electric charge passed during the test and that equivalent to the amount of loaded MOX.

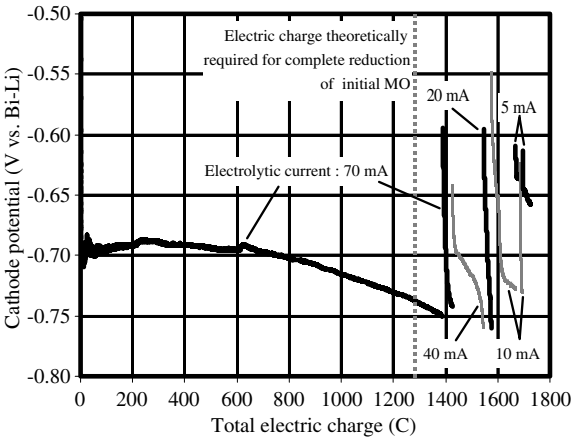

Fig. 6. Change of the cathode potential during the second electrochemical reduction test.

completed and lithium ion in the electrolyte began to be reduced in the first step. This behavior can be used for detection of the MOX reduction. On the other hand, in the sixth and eighth steps, where only 5 mA was applied, the cathode potential did not decrease beyond −0.70 V. It is considered that 5 mA is too small to go over the deoxidization of tantalum which was seen only very slightly in the cyclic voltammetry.

The anode potential was kept below the limiting value (+2.0 V) during most of the test period. After all the electrochemical reduction tests, a little amount of yellow deposit was found on the surface of the platinum anode. It is considered to be Li_2PtO_3 produced by the following reaction:

$$Pt + 2Li^+ + 3O^{2-} = Li_2PtO_3 + 4e^- \quad (5)$$

This is the same behavior as seen in the previous studies with uranium oxide [11]. Since consumption of the platinum metal anode by this reaction seems unavoidable under the condition where the oxygen ion is oxidized in the reaction (2), it is necessary to find adequate design and conditions to keep the progress of the reaction (5) as slow as possible.

3.3. Evaluation of reduced ratio by mass change of samples

Since the cathode products were accompanied with lithium chloride electrolyte and stuck in the tantalum basket, they were washed with 20–30 ml of methanol. The lithium chloride quickly dissolved in methanol. During the washing of the product from the first electrochemical reduction test, small bubbles were generated from the reduction product and a little amount of black powder precipitated. Because these bubbles and black powder were likely to be products from oxidation of actinide metals by methanol, the washing was finished as soon as possible after the reduction products were released from the tantalum basket for the second time. Consequently, no precipitate was observed in washing the product of the second test. After the washing, lithium chloride was completely removed from the surface of the reduction products and the tantalum basket. Major portion of the surface of the first reduction product was black most probably due to oxidation by methanol, although there were also some small spots of metallic shine. Most part of the surface of the reduction product of the second test was free from oxidation and shiny as shown in Fig. 7, owing to the minimum washing time.

The weights of the reduction products after the washing with methanol, together with those before reduction, are shown in Table 4. By comparison between the actual weight of the reduction product and that theoretically calculated assuming 100% reduction, the reduced ratio of each sample can be evaluated. Thus calculated reduced ratio for the samples from the first electrochemical reduction test were estimated as over 100%. This result comes from the underestimated weight of the product probably due to the loss from the black precipitation formed during the washing with methanol. On the other hand, the reduced ratio was evaluated to be nearly 100% for the product from the second electrochemical reduction test from which significant amount of the precipitate was not generated in the washing step. Putting those findings together, the actual reduced ratio under the conditions

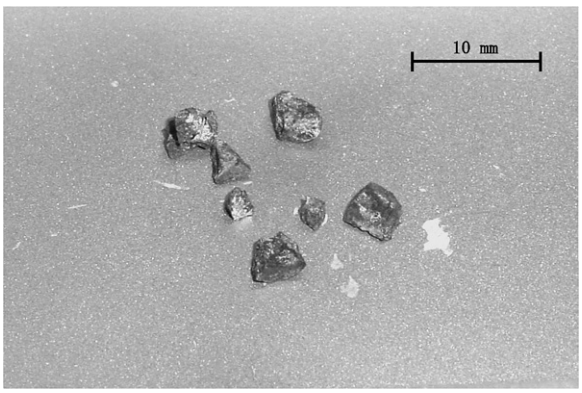

Fig. 7. View of the reduction product of the second electrochemical reduction test.

Table 4
Reduced ratio of the reduction products evaluated from the weight change during the electrochemical reduction

Run no.		Weight before reduction (g)	Weight of the product after wash (g)	Theoretical weight of the product after 100% reduction (g)	Evaluated reduced ratio (%)
1	Piece 1	0.1956	0.165	0.172	132.0
	Piece 2	0.1314	0.109	0.116	143.8
	Total	0.3270	0.274	0.288	136.8
2	Total	0.8906	0.788	0.785	97.2

adopted in this study can be concluded approximately 100%. The reduced ratio evaluated in this manner, however, is one of the feasible choices and could give large error derived from washing and weighing steps. Combination of other methods, such as chemical analysis or measurement of hydrogen gas evolved by reaction with acid solution (gas-burette method [4]), is then necessary to improve the accuracy and reliability of the results.

With the ratio between the total electric charge actually passed during the electrochemical reduction tests and the theoretically required charge for the complete reduction (shown in Table 3), the cathodic current efficiency is evaluated to be 38.9% and 74.6% for the first and second tests, respectively. The reason for this low current efficiency is the consumption of the cathodic current by the deoxidization of tantalum and the reduction of lithium in the electrolyte.

3.4. SEM/EDX analysis of reduction products

Small samples were taken from the initial Np-MOX pellet and the reduction products of the two electrochemical reduction tests. After polishing, these samples were submitted to the observation by scanning electron microscope (SEM) and the energy dispersion X-ray (EDX) analysis.

Fig. 8 shows the secondary electron image (SEI) taken from the central part of the initial Np-MOX pellet. It can be seen that this material has high density and excellent homogeneity. EDX spectrum was also taken for this sample. Because there is too much interference among the Mα lines by the actinide elements, the peak counts of the Lα lines are used in the following quasi-quantitative considerations. As shown in Table 5, the ratio between the peak counts from uranium and plutonium (1.34) agrees with the value calculated from the composition of the pellet (1.33, from Table 2) determined by the

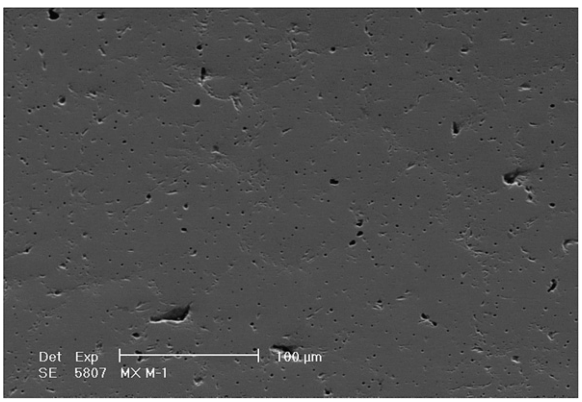

Fig. 8. SEI of the central part of the initial Np-MOX pellet.

Table 5
Composition of the initial Np-MOX and the reduction determined by EDX point analysis (in at.%)

	Determined by chemical analysis	Determined by EDX analysis			
	Initial Np-MOX	Initial Np-MOX	Product from run-1	Product from run-2 (1)	Product from run-2 (2)
U	53.96	48.88	49.36	48.12	48.05
Pu	40.44	36.45	34.6	38.67	36.47
Np	5.07	14.67	16.04	13.12	15.48
U/Pu	1.33	1.34	1.43	1.24	1.32
U/Np	10.64	3.33	3.08	3.67	3.10

chemical analysis. Because the peaks of uranium and plutonium significantly interfere with the count from neptunium, and because it is difficult to compensate the contribution by the relaxation from the excitation after α-decay of neptunium-237, the quantitative evaluation of neptunium concentration from the single EDX spectrum was not possible. There was no significant change of the above U/Pu peak count ratio throughout the whole sample.

Fig. 9 shows the SEM image of whole sample from the reduction product of the second electrochemical reduction test. The sample is clearly a part of the annular shape and its thickness is approximately same as that of the initial Np-MOX pellet before reduction. Closer observation shows that the density of the reduced sample varies with the location. Generally, the density is higher near the surface of the sample and lower around the center. Typical examples of those regions are shown in Figs. 10 and 11, respectively. It can be seen that cohesion among the reduced metal grains proceeded much more in the surface region of the sample, which consequently leaded to the higher density. In the central region, on the other hand, the unit structure of dimension of around 10 μm, which is the average grain size in the original Np-MOX pellet, is still observed. It indicates connection among the metal grains scarcely progressed in that region. Such distribution of the density in the reduction products might be explained by the difference in the period to be at high temperature after the electrochemical reduction. Since the reduction proceeds from the peripheral part of the material, the reduced metal in the surface region remains at the experimental temperature longer than that in the central part which is reduced later at the end of the tests.

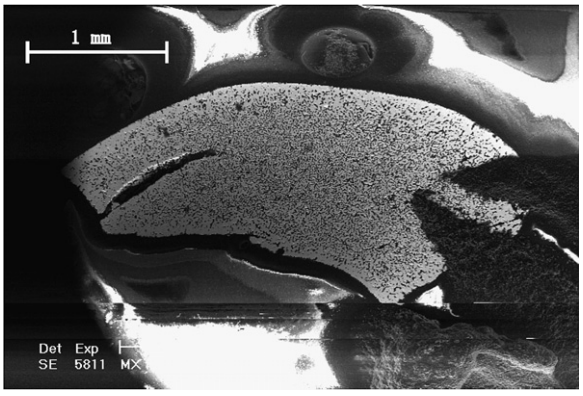

Fig. 9. SEI of whole sample from the reduction product of the second electrochemical reduction test.

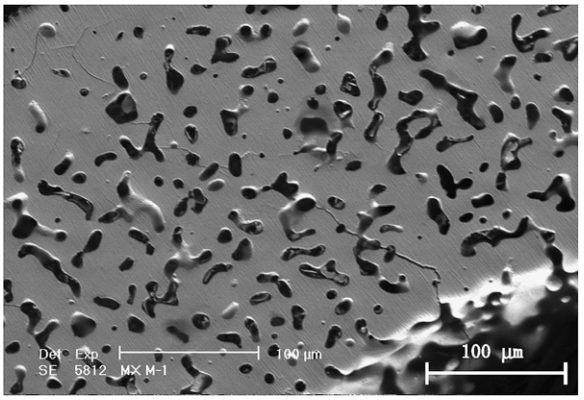

Fig. 10. SEI of surface part of reduction product of the second electrochemical reduction test.

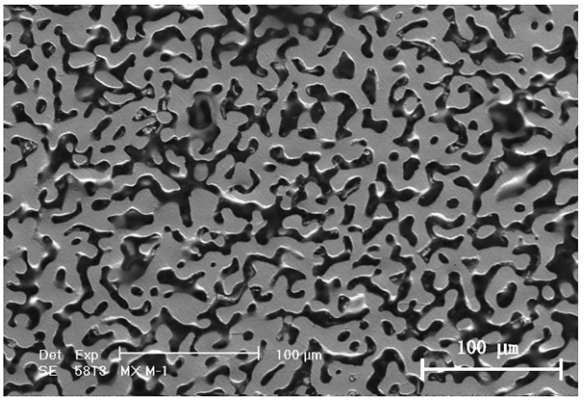

Fig. 11. SEI of central part of reduction product of the second electrochemical reduction test.

The composition of the reduction products determined by EDX spectrum measured at some points is shown in Table 5 as well as the value for the initial Np-MOX. The ratio among the content of uranium, plutonium and neptunium shows little difference from that in the initial Np-MOX pellet. Therefore, the change of the actinide composition in the cathode during the electrochemical reduction is considered very small, if there is any. Mapping by EDX was also made for uranium, plutonium and neptunium indicating no segregation of these elements in the reduction products.

3.5. Behavior of actinide elements in electrochemical reduction – chemical composition of reduction products

The chemical composition of the reduction products determined by ICP-MS is shown in Table 6.

Table 6
Chemical composition of the reduction products determined by ICP-MS (wt ppm)

	Product from run-1	Product from run-2
Mg	7.38×10^0	2.39×10^0
Ta	6.526×10^1	1.645×10^1
Pt	2.45×10^2	1.535×10^0
Np	3.394×10^4	4.040×10^4
U	3.575×10^5	4.240×10^5
Pu	2.511×10^5	3.075×10^5
Am	6.481×10^3	7.379×10^3

The concentrations of the impurities (Mg, Ta, Pt) are very low compared to those of the actinides, although the reason is not yet clear why those impurities show larger discrepancies between the results from two samples compared to the actinide elements. It is most likely that all these impurities come into the product by physical entrainment. Tantalum should be from the electrode/basket material and platinum might be from Li_2PtO_3 peeled off from the anode. The atomic ratio among the actinides in the reduction products seems almost the same as that in the initial Np-MOX. More quantitative comparison was made by defining 'enrichment' factor as follows:

Enrichment of actinide M
= (concentration of M/that of uranium in the reduction product)/(concentration of M/that of uranium in the initial MOX).

This 'enrichment' factor larger than unity indicates that the actinide of interest is somehow concentrated in the reduction product. Although the calculated factors ranged within 5% around unity as shown Fig. 12, no evident dependence on the elements was distinguished. If there is any tendency, it should be too weak compared to the error that ordinarily occurs in chemical analyses.

3.6. Behavior of actinide elements in electrochemical reduction – change of molten salt electrolyte composition

The molten lithium chloride electrolyte was sampled before Li_2O addition (called 'blank LiCl' hereafter) and after each electrochemical reduction test. The composition of the samples was analyzed by ICP-MS as shown in Table 7. Magnesium and platinum in the salt clearly inevitably came from the crucible and the electrode materials, respectively.

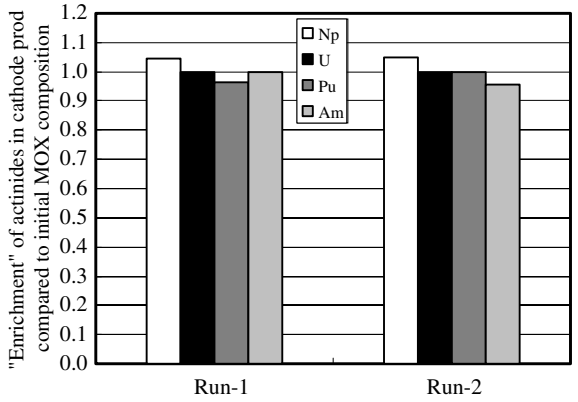

Fig. 12. 'Enrichment factor' of actinides in the reduction products.

Table 7
Chemical composition of the salt samples determined by ICP-MS (wt ppm)

	After run-1	After run-2
Mg	2.73	1.78
Ta	44.62	15.27
Pt	0.02	3.05
Np	0.16	0.11
U	0.33	1.17
Pu	2.61	4.53
Am	0.45	1.82

Since the concentration of platinum is a little higher than expected from its thermodynamic stability, a little amount of Li_2PtO_3 might be flaked off from the anode and physically entrained into the sample. Tantalum is also considered to come from the electrode material, since its potential was sometimes scanned to the range high enough to lead it to get oxidized.

The change of the actinide concentrations is plotted in Fig. 13. Though the absolute values are very small, the actinide concentrations increased according to the progress of the tests. To illustrate the difference among the behaviors of these elements clearer, the 'enrichment' factor of each actinide against uranium was calculated as well as in the case of the reduction products (Fig. 14).

Enrichment of actinide M
= (concentration of M/that of uranium in the salt)/(concentration of M/that of uranium in the initial MOX).

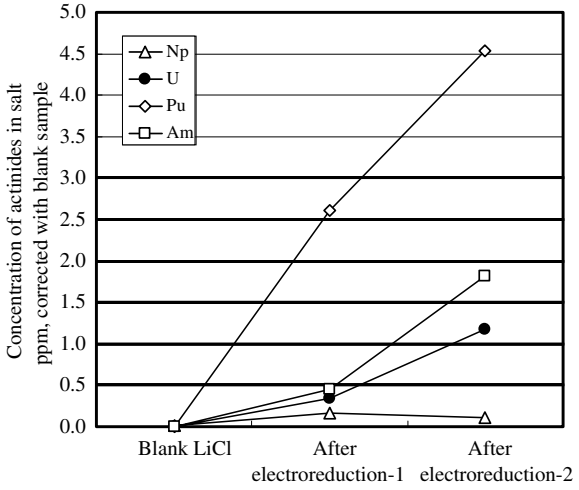

Fig. 13. The change of the actinide concentrations in the salt samples.

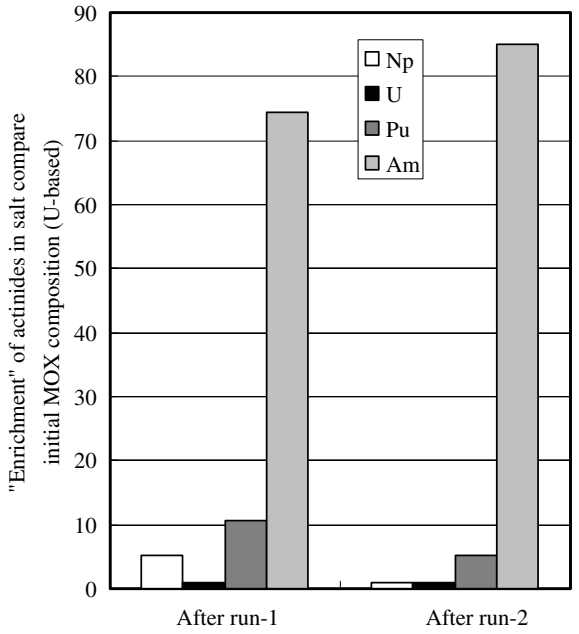

Fig. 14. 'Enrichment factor' of actinides in the salt samples.

It is obviously seen that the 'enrichment' factor of plutonium and americium are much larger than that of neptunium. It indicates that the detected actinides in the salt samples are neither the MOX nor the reduced particle that fell down from the cathode, because the composition of the actinides in the salt samples was much different from that in the initial Np-MOX. It is also suggested that plutonium and americium tend to distribute in the salt phase in relatively higher ratios compared with those for uranium and neptunium. In the previous study on the lithium reduction process, it has been reported that lanthanide oxides could not be reduced and that these elements easily dissolved into the lithium chloride melt as their oxychloride forms at higher Li_2O concentration [6]. Since the transuranium and the lanthanide elements have, in general, very similar chemical characteristics, it is quite likely that plutonium and americium dissolve into the melt in the same manner. Because the absolute concentrations of the actinides are very low in the present study, it is difficult to enter further discussion. More dedicated experiments are needed to clarify the chemical behavior of the actinides, such as chemical form, distribution factor, solubility, and so on in circumstances for the electrochemical reduction.

4. Conclusions

It is necessary to understand the behavior of minor actinide and major fission product elements in the electrochemical reduction process in order to evaluate the material balance and to establish the process flow sheet of the electrochemical reduction process for oxide nuclear fuels. In the present study, the electrochemical reduction of $(U–40Pu–5Np)O_2$ was performed in molten lithium chloride melt at 923 K to investigate fundamental behavior of the transuranium elements and applicability of the method to reduction process for these materials.

From the results of current–potential curve measurement with the MOX, it was indicated that the MOX was electrochemically reduced at the potential lower than −0.6 V vs. Bi–35 mol% Li reference electrode. In the electrochemical reduction at stepwise electric current, the end point of MOX reduction could be detected by the quick downward change of the cathode potential indicating the exhaustion of MOX and the reduction of lithium ion in the electrolyte.

The reduced metal grains in the surface region of the sample cohered each other and made the layer of relatively high density, although it did not prevent the reduction of the sample to the center. Complete reduction of the MOX was suggested by the weight change through the electrochemical reduction and SEM–EDX observation. The chemical composition of the reduction products was homogeneous and identical to that of initial Np-MOX, also indicating

that the reduction was completed and not selective among the actinides.

The concentration of the actinide elements, especially plutonium and americium, increased according to the progress of the tests, although their absolute values are very small. It is quite likely that plutonium and americium dissolve into the melt in the same manner as the lanthanide elements in the lithium reduction process. Dedicated experiments are needed to determine the chemical form, solubility in the electrolyte and the dissolved ratio of the actinides correlated with the operating conditions of the electrochemical reduction such as the processing duration and the concentration of Li_2O in the electrolyte.

Acknowledgements

The authors gratefully appreciate Drs J.P. Glatz, T. Wiss, D. Cromboom and Messrs. M. Ougier, A. Rodorigues for their kind support and experienced analytical works which enabled these experiments. This work was supported by MEXT (Ministry of Education, Culture, Sports, Science and Technology of Japan), Development of Innovative Nuclear Technologies Program 'Development of Electrochemical Reduction Process for Oxide Nuclear Fuel'.

References

[1] T. Inoue, T. Yokoo, T. Nishimura, in: International Conference on Future Nuclear Systems, Global'99, Jackson Hole, WY, August 29–September 3, 1999.
[2] T. Koyama, M. Iizuka, Y. Shoji, R. Fujita, H. Tanaka, T. Kobayashi, M. Tokiwai, J. Nucl. Mater. 34 (1997) 384.
[3] T. Usami, M. Kurata, T. Inoue, H.E. Sims, S.A. Beetham, J.A. Jenkins, J. Nucl. Mater. 300 (2002) 15.
[4] T. Kato, T. Usami, M. Kurata, T. Inoue, H.E. Sims, J.A. Jenkins, CRIEPI Report T01003, 2001 (in Japanese).
[5] T. Usami, T. Kato, M. Kurata, T. Inoue, H.E. Sims, S.A. Beetham, J.A. Jenkins, J. Nucl. Mater. 304 (2002) 50.
[6] T. Kato, T. Usami, R. Yuda, M. Kurata, H. Moriyama, CRIEPI Report T99009, 2000 (in Japanese).
[7] A. Kawabe, T. Kato, M. Kurata, CRIEPI Report T02041, 2003 (in Japanese).
[8] K. Gourishankar, L. Redey, M. Williamson, in: W. Schneider (Ed.), Light Metals 2002, TMS, 2002, p. 1075.
[9] M. Kurata, T. Inoue, J. Serp, M. Ougier, J.P. Glatz, J. Nucl. Mater. 328 (2004) 97.
[10] M. Kurata, Y. Sakamura, T. Omori, T. Inoue, Electrochem. Acta, in press.
[11] Y. Sakamura, M. Kurata, T. Inoue, J. Electrochem. Soc. 153 (D31) (2006).